Synthesis and Structure of and Cation Distribution in the Zirconium Cluster Rb[(Zr$_6$C)Cl$_{15}$]

Henning W. Rohm and Martin Köckerling

University of Rostock, Department of Chemistry, Inorganic / Solid State Chemistry Group,
Albert-Einstein-Straße 3a, D-18059 Rostock, Germany

Reprint requests to Prof. Dr. Martin Köckerling. Fax: +49-381-498-6382.
E-mail: Martin.Koeckerling@uni-rostock.de

Dedicated to Professor Dr. Dr. h. c. mult. Rudolf Hoppe on the occasion of his 85th birthday

Rb[(Zr$_6$C)Cl$_{15}$] was prepared by heating ZrCl$_4$, Zr powder, RbCl and Al$_4$C$_3$ at 850 °C for 21 days. The crystal structure was determined by single crystal X-ray diffraction (space group *Pmma*, $a =$ 18.484(3), $b =$ 18.962(2), $c =$ 9.708(1) Å, $V =$ 2505.4(6) Å^3, and $Z =$ 4). Rb[(Zr$_6$C)Cl$_{15}$] crystallises in the Cs[Nb$_6$Cl$_{15}$]-type structure. It is built up from two interconnected types of cluster chains, one with linear Zr−Cl$^{a−a}$−Zr bridges, the other one with bent bridges. The rubidium cations are spread over three different sites within the cluster network which differs significantly from the cation distribution in the comparable potassium and caesium phases. The cation distribution can be rationalised considering the size of the cavities and the Coulombic interactions.

Key words: Zirconium, Halide, Solid State, Cluster, Crystal Structure

Introduction

A prolific cluster chemistry of reduced ternary and quaternary zirconium halides is accessible through methods of high-temperature solid-state chemistry [1 – 5]. Almost all of these phases contain octahedra of zirconium atoms centred by an interstitial atom Z, with Z including H, Be–N, Al–P, and Mn–Ni. These compounds have the general formula $A_x^{I,II}[(Zr_6Z)X_{12}{}^i X_n{}^a]$, with $A^{I,II} =$ alkali or alkaline earth metal cation, $X =$ Cl, Br or I, $X^i = inner$, edge-bridging halide [6], $X^a = outer$, exo-bonded halide, and $0 \leq x, n \leq 6$. With different cations, interstitial atoms, and different values of x and n, a large variety of (in most cases) network structures has been established. So far, chlorides and bromides have been found for $n = 0–6$; whereas iodides are limited to $n = 0$ and 2 [1 – 4].

Phases with $n = 3$ are a structurally interesting series because all the outer halide atoms in each cluster are shared as $(X^{a−a})_{6/2}$ between neighbouring cluster units. So far, a total of 6 independent cluster network types exist with this type of inter-cluster connectivity. They differ in terms of $(−Zr−Cl^{a−a}−Zr−)$ ring sizes, second-nearest neighbour cluster interconnections, and angles at $X^{a−a}$ as well as in the range of sites for any counter cations [7, and refs. cited therein]. Besides the

members of the 6 parent structures, further examples exist with mixed halides [8], and also with distorted versions of the more symmetrical archetypes [9].

In this paper we report about a modified synthesis and the single crystal structure of Rb[(Zr$_6$C)Cl$_{15}$].

Results and Discussion

The title phase, Rb[(Zr$_6$C)Cl$_{15}$], was obtained as a product of the reaction of stoichiometric amounts of ZrCl$_4$, Zr powder, RbCl, and Al$_4$C$_3$ at 850 °C, according to

$$27\,ZrCl_4 + 9\,Zr + 6\,RbCl + 2\,Al_4C_3$$
$$\rightarrow 6\,Rb[(Zr_6C)Cl_{15}] + 8\,AlCl_3$$
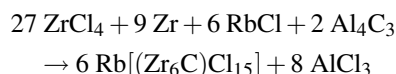
We assume, that the byproduct AlCl$_3$ serves as flux and improves crystallinity. Rb[(Zr$_6$C)Cl$_{15}$] forms black crystals which turn dark red-brown on grinding. The Guinier powder patterns of different reaction products, obtained from a Rb : Zr ratio of 1 : 6 did not show any lines of other cluster phases, but eventually weak lines of non-cluster phases, for example of Rb$_2$[ZrCl$_6$] [10]. Rb[(Zr$_6$C)Cl$_{15}$] crystallises in the orthorhombic space group *Pmma* (no. 51) with $a =$ 18.484(3), $b =$ 18.962(2), $c =$ 9.708(1) Å, $V =$

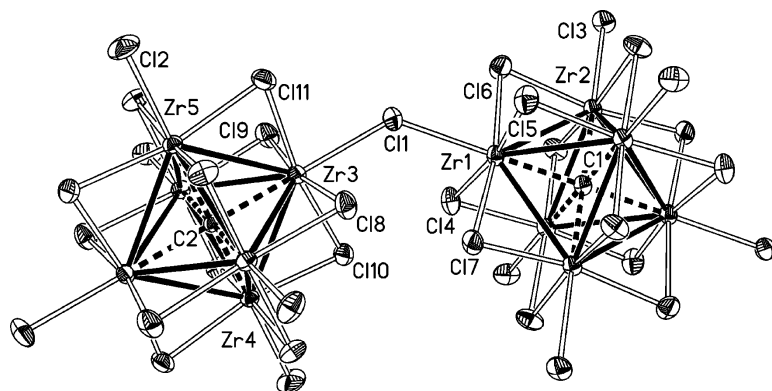Fig. 1. View of the two symmetry-independent cluster units in Rb[(Zr$_6$C)-Cl$_{15}$] with atom numbering scheme (displacement ellipsoids at the 50 % probability level; Zr–Zr bonds emphazised).

Table 1. Crystal structure data for Rb[(Zr$_6$C)Cl$_{15}$].

	Rb[(Zr$_6$C)Cl$_{15}$]
Formula	CCl$_{15}$RbZr$_6$
M_r	1176.55
Cryst. size, mm^3	$0.51 \times 0.41 \times 0.32$
Crystal system	orthorhombic
Space group	*Pmma*
a, Å	18.484(3)
b, Å	13.962(2)
c, Å	9.708(1)
V, Å^3	2505.4(6)
Z	4
D_{calcd}, g·cm^{-3}	3.12
$\mu(MoK_\alpha)$, mm^{-1}	59.2
$F(000)$, e	2152
hkl range	$-1 \rightarrow 26, -19 \rightarrow 1, -13 \rightarrow 1$
$((\sin\theta)/\lambda)_{max}$, Å^{-1}	0.70
Refl. measured	4849
Refl. unique	3885
R_{int}	0.020
Param. refined	135
$R(F)/wR(F^2)^a$ (all refls.)	0.036 / 0.097
GoF $(F^2)^b$	1.143
$\Delta\rho_{fin}$ (max/min), e Å^{-3}	1.738 / -1.24

^{a} $R = \sum_{hkl} ||F_o| - |F_c|| / \sum_{hkl} ||F_o|$; $wR = \left(\sum_{hkl} w(F_o^2 - F_c^2)^2 / \sum_{hkl} w(F_o^2)^2\right)^{1/2}$; $w = 1/[\sigma^2(F_o^2) + (0.0440P)^2 + 8.7497P]$ where $P = (F_o^2 + 2F_c^2)/3$; ^{b} GoF $= \sum_{hkl} w \left(||F_o^2| - |F_c^2||\right)^2 / (m-n)$ where m = number of observed reflections and n = number of parameters.

2505.4(6) Å^3, and $Z = 4$. Some important parameters of the data collection and structure refinement are listed in Table 1. The positional and equivalent isotropic displacement parameters are listed in Tables 2 and 3. This phase was identified previously by J. D. Corbett *et al.* with the aid of Guinier powder diagrams [11]. With a single crystal X-ray structure determination, as presented in this paper, it is possible to determine the distribution of the cations precisely [12].

Within the cluster halides with octahedral hexazirconium units the group with the metal to halide ratio of 6 : 15 offers the largest variety of different structure types. In all cases three-dimensional networks are found with the Zr clusters connected only by X^{a-a} bridges. So far, six independent structure types have been established [7]. Besides members of the [Nb$_6$F$_{15}$] structure [13], realised for example in [(Zr$_6$Co)Cl$_{15}$] [14] with only linear Zr–Cl^{a-a}–Zr bridges, three different structure types exist with exclusively bent bridges, namely (1) [Ta$_6$Cl$_{15}$] [15] (examples: [(Zr$_6$N)Cl$_{15}$] and Na$_{0.5}$[(Zr$_6$N)Cl$_{15}$] [16]) (2) Rb$_5$[(Zr$_6$Be)Br$_{15}$] [17] (example besides the parent structure: Cs$_3$[(Zr$_6$Z)Br$_{15}$] (Z = B, C) [18]), and (3) Cs[ZrCl$_5$]·Cs$_2$[(Zr$_6$Mn)Cl$_{15}$] [19] (examples besides the parent structure: Cs[ZrCl$_5$]·Cs$_2$[(Zr$_6$B)Cl$_{15}$] and Cs[ZrCl$_5$]·Cs$_2$[(Zr$_6$B)Cl$_{14..6}$I$_{0.4}$] [8]). The two remaining independent structure types contain both linear and bent Zr–Cl^{a-a}–Zr bridges. These are the K$_2$[(Zr$_6$B)Cl$_{15}$] [9] (for example: K$_3$[(Zr$_6$Be)Cl$_{15}$] [9]) and the Cs[Nb$_6$Cl$_{15}$] structure types [20] (examples: K[(Zr$_6$C)Cl$_{15}$] [11], Cs[(Zr$_6$C)Cl$_{15}$] [11, 12], CsK[(Zr$_6$B)Cl$_{15}$] [11], and K[(Zr$_6$N)Cl$_{15}$] [21]). The title phase belongs to the latter structure type.

In the Cs[Nb$_6$Cl$_{15}$] structure two different types of cluster chains exist. One is a linear chain, which runs parallel to the crystallographic c axis. The other one runs along the a axis and contains bent Zr–Cl^{a-a}–Zr bridges, thereby forming zigzag chains. The two symmetry-independent cluster units, from which these two chains originate, are shown in Fig. 1. Fig. 2 shows the arrangement of the two cluster chains in the unit cell. The Zr$_6$ octahedra of the linear chains are tetragonally compressed along the c axis by 0.05 Å with an average Zr–C distance of 2.241 Å along, and 2.291 Å perpendicular to the chain direction. The metal octahedra of the zigzag chains are also tetragonally compressed by about 0.03 Å in the chain direction

Atom	x	y	z	U_{eq}	Occupancy
C1	1/2	1/2	1/2	0.013(1)	1
C2	1/4	0	0.1614(8)	0.011(1)	1
Cl1	0.43768(6)	0.25061(8)	0.1613(1)	0.0235(2)	1
Cl2	1/4	0	−0.3381(2)	0.0289(5)	1
Cl3	3/4	1/2	0.3163(2)	0.0200(4)	1
Cl4	1/2	0.2465(1)	1/2	0.0214(3)	1
Cl5	0.43354(9)	1/2	0.1562(2)	0.0231(3)	1
Cl6	0.59504(5)	0.37253(8)	0.2360(1)	0.0220(2)	1
Cl7	0.33962(5)	0.37456(7)	0.4187(1)	0.0201(2)	1
Cl8	1/4	0.2543(1)	0.1552(2)	0.0213(3)	1
Cl9	0.44251(8)	0	0.1627(2)	0.0224(3)	1
Cl10	0.34569(6)	0.12636(8)	0.4217(1)	0.0200(2)	1
Cl11	0.34757(6)	0.12631(8)	−0.0975(1)	0.0205(2)	1
Rb1	1/4	1/2	0.10(1)	0.27(6)	0.08(1)
Rb2	1/2	0	1/2	0.06(2)	0.028(6)
Rb3	1/4	0.25239(5)	0.67352(8)	0.0316(3)	0.963(3)
Zr1	0.46986(2)	0.38438(3)	0.34324(4)	0.0135(1)	1
Zr2	0.61407(3)	1/2	0.41778(6)	0.0131(1)	1
Zr3	0.33776(2)	0.11587(3)	0.16234(4)	0.0130(1)	1
Zr4	1/4	0	0.39233(8)	0.0121(2)	1
Zr5	1/4	0	−0.06921(8)	0.0130(2)	1

Table 2. Atomic coordinates, equivalent isotropic displacement parameters (U_{eq}, Å^{-2}) and occupancies for Rb[(Zr$_6$C)Cl$_{15}$] with estimated standard deviations in parentheses.

Atom	U_{11}	U_{22}	U_{33}	U_{23}	U_{13}	U_{12}
C1	0.009(3)	0.012(3)	0.016(4)	0	−0.002(3)	0
C2	0.013(3)	0.010(3)	0.009(3)	0	0	0
Cl1	0.0225(5)	0.0230(5)	0.0250(5)	−0.0071(4)	0.0040(4)	−0.0102(4)
Cl2	0.041(1)	0.036(1)	0.0099(9)	0	0	0
Cl3	0.0101(8)	0.024(1)	0.026(1)	0	0	0
Cl4	0.0215(7)	0.0141(6)	0.0288(7)	0	−0.0066(6)	0
Cl5	0.0272(7)	0.0215(7)	0.0204(7)	0	−0.0074(6)	0
Cl6	0.0139(4)	0.0254(5)	0.0267(5)	−0.0086(4)	0.0025(4)	−0.0011(4)
Cl7	0.0112(4)	0.0212(5)	0.0278(5)	−0.0058(4)	−0.0003(4)	−0.0034(3)
Cl8	0.0190(6)	0.0138(6)	0.0310(8)	−0.0015(6)	0	0
Cl9	0.0120(6)	0.0225(7)	0.0327(8)	0	0.0005(6)	0
Cl10	0.0214(5)	0.0227(5)	0.0161(4)	−0.0033(4)	−0.0014(4)	−0.0074(4)
Cl11	0.0215(5)	0.0241(5)	0.0159(4)	0.0030(4)	0.0016(4)	−0.0065(4)
Rb1	0.12(4)	0.08(3)	0.6(2)	0	0	0
Rb2	0.07(4)	0.07(4)	0.05(3)	0	−0.02(3)	0
Rb3	0.0316(4)	0.0270(4)	0.0361(4)	0.0081(3)	0	0
Zr1	0.0093(2)	0.0130(2)	0.0182(2)	−0.0017(1)	−0.0009(1)	−0.0009(1)
Zr2	0.0074(2)	0.0135(2)	0.0184(3)	0	−0.0003(2)	0
Zr3	0.0122(2)	0.0133(2)	0.0135(2)	−0.0002(1)	0.0000(1)	−0.0022(1)
Zr4	0.0129(3)	0.0137(3)	0.0098(3)	0	0	0
Zr5	0.0147(3)	0.0147(3)	0.0095(3)	0	0	0

Table 3. Anisotropic displacement parameters (Å^{-2}) for Rb[(Zr$_6$C)Cl$_{15}$] with estimated standard deviations in parentheses.

with Zr−C distances of 2.2546(6) and 2.2873(4) Å. The Zr–Cl^{a-a}–Zr-angle of the zigzag chains measures 137.19(9)°. The three-dimensional cluster network is formed by additional Cl^{a-a} bridges between the two different chain types with Zr–Cl^{a-a}–Zr-angles of 131.34(4)°. Within this cluster network cavities exist, in which the alkali cations are accommodated. As can be seen from the data in Table 4, which compares the structural data of the title phase with those of the homeotypic compounds K[(Zr$_6$C)Cl$_{15}$] [11] and Cs[(Zr$_6$C)Cl$_{15}$] [11, 12], the Zr1–Cl1–Zr3 and Zr2–Cl3–Zr2$^{\#}$ angles (symmetry operation #: –x+3/2, 1–y, z) are expanded with increasing cation size. Thereby, the cavities, which host the cations within the cluster network, are expanded and adapted to the size of cation. From the other members of this structure type it is known already [11] that three different network cavities are used by the cations. These are the Wyckoff sites 4k, 2f, and 2c of the space group $Pmma$. Regarding the question what type of cation takes which site, the size and the bonding capabilities of the cation are the most important parameters. Whereas in K[(Zr$_6$C)Cl$_{15}$] the

Table 4. Selected bond lengths (Å), angles (deg), and dihedral angles (deg) for K[(Zr$_6$C)Cl$_{15}$], Rb[(Zr$_6$C)Cl$_{15}$], and Cs[(Zr$_6$C)Cl$_{15}$] with estimated standard deviations in parentheses[a].

	K[(Zr$_6$C)Cl$_{15}$]	Rb[(Zr$_6$C)Cl$_{15}$]	Cs[(Zr$_6$C)Cl$_{15}$]
Zr1–C1	2.2916(5)	2.2873(4)	2.2871(6)
Zr2–C1	2.2571(7)	2.2546(6)	2.2682(7)
Zr3–C2	2.2949(5)	2.2910(4)	2.2883(6)
Zr4–C2	2.247(6)	2.242(8)	2.27(1)
Zr5–C2	2.238(6)	2.239(8)	2.23(1)
Zr1–Cl1	2.639(1)	2.639(1)	2.660(2)
Zr3–Cl1	2.632(1)	2.636(1)	2.649(2)
Zr4–Cl2	2.608(2)	2.617(2)	2.569(3)
Zr5–Cl2	2.598(2)	2.611(2)	2.571(3)
Zr1–Cl1–Zr3	131.02(3)	131.34(4)	132.84(6)
Zr2–Cl3–Zr2[#]	137.04(5)	137.19(9)	137.7(1)
Zr4–Cl2–Zr5	180	180	180

[a] Symmetry code #: $-x + 3/2, -y + 1, z$.
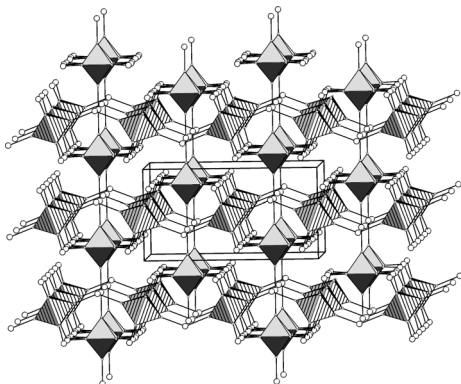

Fig. 2. The arrangement of the linear and bent cluster chains in an expanded view of the unit cell of Rb[(Zr$_6$C)Cl$_{15}$] (inner halides omitted for clarity, view down b, a horizontal).
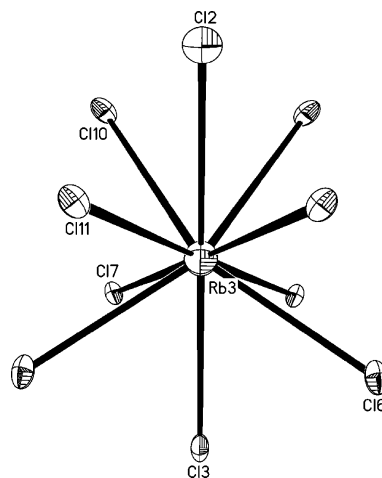

Fig. 3. The halide environment of the Rb3 cation, located on the Wyckoff site $4k$ (displacement ellipsoids at the 50 % probability level).
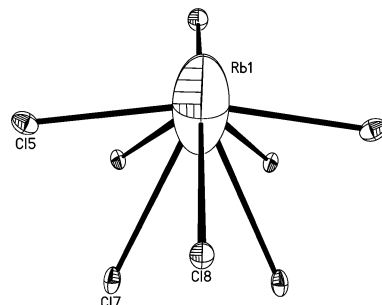

Fig. 4. The halide environment of the Rb1 cation, located on the Wyckoff site $2f$ (displacement ellipsoids at the 50 % probability level).
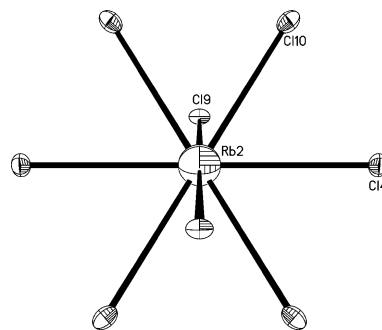

Fig. 5. The halide environment of the Rb2 cation, located on the Wyckoff site $2c$ (displacement ellipsoids at the 50 % probability level).

$4k$ site is exclusively occupied by the K cation [11], in the Rb and Cs salts the cations also use the $2f$ and $2c$ sites. When these two additional sites are occupied, an interesting interplay takes place between the size requirements of the cations and the Coulomb interactions between the cations and the surrounding halide ions. This interplay can be illustrated by a comparison of the structural data of the K, Rb, and Cs cluster salts, which are compiled in Tables 4 and 5.

As already mentioned above, the cation in K[(Zr$_6$C)Cl$_{15}$] occupies exclusively the Wyckoff site $4k$ with a coordination polyhedron consisting of 10 Cl atoms forming a distorted, doubly capped cube. The average Cl–K distance measures $\bar{d} = 3.419$ Å, a value which compares well with the sum of the ionic radii (3.40 Å [21], Shannon values). Changing to the heavier rubidium cation the $4k$ cavity size increases slightly. It is occupied by the Rb3 cation, which has a coordina-

tion environment shown in Fig. 3. Even though the size of this cavity with $\bar{d}$(Rb–Cl) = 3.431 Å (average) is slightly smaller than the sum of the ionic radii (3.47 Å), the almost full occupation of this site shows that it is

Table 5. Comparison of the Cl–M bond lengths of the compounds M[(Zr$_6$C)Cl$_{15}$] with the sums of ionic radii R for M = K, Rb, or Cs[a].

Position	CN	$\bar{d}$(Cl–M) (Å)	R (Å)	X (%)	$\bar{d}$(Cl–M) (Å)	R (Å)	X (%)	$\bar{d}$(Cl–M) (Å)	R (Å)	X (%)
		— M = K —			— M = Rb —			— M = Cs —		
2c	8	–	3.32	0	3.440(1)[b]	3.42	1.4(4)	3.498(4)[b]	3.55	45(2)
2f	8	–	3.32	0	3.70(5)	3.42	3.8(4)	3.87(3)	3.55	50(2)
4k	10	3.419(2)	3.40	100	3.431(1)	3.47	94.8(4)	3.408(6)	3.62	5.0(2)

[a] $R = \sum r_{Cl^-, M^+}$; X = percentage of the overall halide contents; distances to the 2c position; [b] the refinement was carried out with a split model with an occupied 4i position instead of the 2c position.

large enough for the rubidium cation. Interestingly, in the caesium phase the average Cs–Cl distance is not larger than in the Rb phase, but smaller by 0.023 Å. Comparison of the average Cs–Cl distance (3.408 Å) with the sum of the ionic radii of ten-fold coordinated Cs$^+$ (3.62 Å) shows that the site 4k is too small to accommodate larger amounts of Cs. Therefore, only 5 % of the total caesium content of this phase is found on the 4k site. The coordination environment of the Rb1 cation on the site 2f is shown in Fig. 4, that of Rb2 on the Wyckoff site 2c in Fig. 5. Both cations are surrounded by 8 chlorine atoms. In Cs[(Zr$_6$C)Cl$_{15}$] the 2f site is fully occupied. From the comparison of the sum of the ionic (Shannon) radii for a caesium cation with coordination number 8 (3.55 Å) with $\bar{d}$(Cl–Cs) = 3.87(3) Å, it is obvious that there are no size restrictions for a complete occupation of this site. The lower Cs occupation (90 %) of the 2c site is clearly correlated with the shorter average distance $\bar{d}$(Cl–Cs) = 3.498(3) Å. The Cs ion on this site shows an elongated displacement ellipsoid, which was split in the structure refinement into two positions, thereby changing the discussed site to the Wyckoff site 4i.

A similar situation is found in the title phase. The 2f site is occupied with 3.8(4) % of the total Rb content, but to a higher extent than the 2c site, which holds only 1.4(4) % of the cations. This fact cannot be explained solely by the average Rb–Cl distances though, because the comparison of the sum of the ionic radii (3.42 Å) with $\bar{d}$(Cl–Rb) = 3.440 Å shows, that there is no size restriction. Another possible factor that can influence the amount of site occupation, is the coordination geometry and the total Coulomb interaction between the cations and the surrounding anions. When comparing the coordination geometry of Rb2 (Fig. 5) with that of Rb3 (Fig. 3) (coordination number 8 in both cases), it is evident that Rb2 is even less regularly coordinated than Rb3. Whereas Rb2 on the 2c site is surrounded by a ring of Cl atoms, Rb3 (2f site) is covered by a hemisphere of ligand atoms. This more regular environment causes more effective Coulomb interactions

to appear. These interactions can be rationalised using partial Madelung factors (PMF). The calculation of the PMF [22] allows us to estimate the amount of lattice energy, which is released on occupation of this cation site, and gives a value of 0.52863 for the 2c site. It is slightly smaller than the PMF for the 2f site, which calculates to 0.57163. These numbers correlate nicely with the observed occupation of these two cation sites.

Experimental Section

All manipulations were carried out in an argon filled glove box or under high vacuum because of the moisture and air sensitivity of the starting materials and the products. Zr was obtained by a process of hydrogenation, grinding and subsequent dehydrogenation of reactor grade Zr pieces [23, 24].

Al$_4$C$_3$ powder (ABCR, > 99 %) was degassed at 800 °C under high vacuum prior to use. Neither X-ray powder diagrams, nor the colour of this material indicated the presence of nitrogen containing Al phases [25]. ZrCl$_4$ (Aldrich, < 50 ppm Hf, 99.5 %) and RbCl (Alfa Aesar, > 99.9 %) were purified by sublimation under high vacuum.

Synthesis of Rb[(Zr$_6$C)Cl$_{15}$]

Crystals of the title compound were prepared by sealing 233.0 mg (1.000 mmol) of ZrCl$_4$, 30.4 mg (0.373 mmol) of Zr, 62.7 mg (0.519 mmol) of RbCl and 10.7 mg (0.074 mmol) of Al$_4$C$_3$ in a welded niobium ampoule. The vessel was sealed into an evacuated silica ampoule to protect it from oxidation during the reaction. The silica ampoule was placed in a tube furnace. The temperature of the furnace was first raised to 350, and then to 500 and 750 °C. After each increase the temperature was held for at least 24 h. In a final step the temperature was raised to 850 °C and held for 21 d. Subsequently, the reaction container was quenched under water. The product was obtained in form of black crystals.

X-Ray structure determination

Black single crystals of the title compound were selected under a microscope (15× magnification) inside an argon-filled glove box and sealed into thin-walled glass capillaries. X-Ray intensity data were collected at r. t. with a Siemens

P4 four-circle diffractometer with graphite-monochromated MoK_α radiation ($\lambda = 0.71073$ Å).

All processing of the data was carried out using XSCANS 2.0. The structure was solved in the orthorhombic space group *Pmma* (no. 51) using Direct Methods and refined by full-matrix least-squares methods on F^2 using the SHELX-97 program package [26]. The occupational factors of all Rb positions were refined unconstrained.

Further details about the crystal structure investigation may be obtained from Fachinformationszentrum Karlsruhe, 76344 Eggenstein-Leopoldshafen, Germany (fax: +49-7247-808-666; e-mail: crysdata@fiz-karlsruhe.de, http://www.fiz-informationsdienste.de/en/DB/icsd/depot_anforderung.html) by quoting the deposition number CSD-417754.

[1] J. D. Corbett, *J. Alloys Compd.* **1995**, *229*, 10 – 23.

[2] J. D. Corbett in *Modern Perspectives in Inorganic Crystal Chemistry*, (Ed.: E. Parthé), NATO ASI Series C, Kluwer Academic Publishers; Dordrecht, The Netherlands **1992**, pp. 27 – 56.

[3] J. D. Corbett, *J. Chem. Soc., Dalton Trans.* **1996**, 575 – 587.

[4] J. D. Corbett, *Inorg. Chem.* **2000**, *39*, 5178 – 5191.

[5] M. Köckerling, in *Inorg. Chem. in Focus III*, (Eds.: G. Meyer, D. Naumann, L. Wesemann), Wiley-VCH, **2006**, pp. 61 – 77, and refs. cited therein.

[6] H. Schäfer, H.-G. von Schnering, *Angew. Chem.* **1964**, *76*, 833 – 849.

[7] R.-Y. Qi, J. D. Corbett, *Inorg. Chem.* **1995**, *34*, 1646 – 1651.

[8] H. W. Rohm, M. Köckerling, *Z. Anorg. Allg. Chem.* **2003**, *629*, 2356 – 2362.

[9] R. P. Ziebarth, J. D. Corbett, *J. Am. Chem. Soc.* **1988**, *110*, 1132 – 1139.

[10] G. Engel, *Z. Kristallogr.* **1935**, *90*, 341 – 373.

[11] R. P. Ziebarth, J. D. Corbett, *J. Am. Chem. Soc.* **1987**, *109*, 4844 – 4850.

[12] H. W. Rohm, M. Köckerling, *Acta Crystallogr.* **2006**, *C62*, i19–i20.

[13] H. Schäfer, H.-G. von Schnering, K. J. Niehues, H. G. Nieder Vahrenholz, *J. Less-Common Met.* **1965**, *9*, 95 – 104

[14] J. Zhang, J. D. Corbett, *Inorg. Chem.* **1991**, *30*, 431 – 435.

[15] D. Bauer, H.-G. von Schnering, *Z. Anorg. Allg. Chem.* **1968**, *361*, 259 – 276.

[16] R. P. Ziebarth, J. D. Corbett, *J. Less-Common Met.* **1988**, *137*, 21 – 34.

[17] R.-Y. Qi, J. D. Corbett, *Inorg. Chem.* **1995**, *34*, 1646 – 1651.

[18] R. Y. Qi, J. D. Corbett, *Inorg. Chem.* **1995**, *34*, 1657 – 1662.

[19] J. Zhang, J. D. Corbett, *Inorg. Chem.* **1995**, *34*, 1652 – 1657.

[20] R. P. Ziebarth, J. D. Corbett, *J. Am. Chem. Soc.* **1988**, *110*, 1132 – 1139.

[21] a) R. D. Shannon, C. T. Prewitt, *Acta. Crystallogr.* **1969**, *B25*, 925 – 946; b) R. D. Shannon, *Acta. Crystallogr.* **1976**, *A32*, 751 – 767.

[22] a) R. Hoppe, *Angew. Chem.* **1966**, *78*, 52 – 63; b) R. Hoppe, *Angew. Chem.* **1970**, *82*, 1 – 16.

[23] a) M. Köckerling, *Inorg. Chem.* **1998**, *37*, 380 – 381; b) M. Köckerling, *Z. Anorg. Allg. Chem.* **1999**, *625*, 24 – 30.

[24] M. Köckerling, J. B. Willems, P. D. Boyle, *Inorg. Chem.* **2001**, *40*, 1439 – 1444.

[25] F. D. Meyer, H. Hillebrecht in *Ceramics – Processing, Realibility, Tribology and Wear* (Euromat 99, Vol. 12), (Ed.: G. Müller), Wiley-VCH, **2000**, pp. 256 – 260.

[26] G. M. Sheldrick, SHELXS-97 and SHELXL-97, Programs for the Solution and Refinement of Crystal Structures, University of Göttingen, Göttingen (Germany) **1997**.